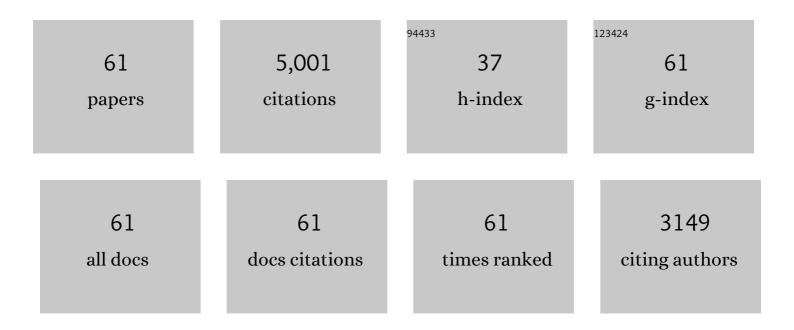
## Hong Wang

List of Publications by Year in descending order

Source: https://exaly.com/author-pdf/860797/publications.pdf Version: 2024-02-01



#	Article	IF	CITATIONS
1	A solid solution-based millimeter-wave absorber exhibiting highly efficient absorbing capability and ultrabroad bandwidth simultaneously <i>via</i> a multi-elemental co-doping strategy. Journal of Materials Chemistry C, 2022, 10, 1381-1393.	5.5	7
2	Wide-bandgap fluorides/polyimide composites with enhanced energy storage properties at high temperatures. Chemical Engineering Journal, 2022, 435, 135059.	12.7	32
3	Significantly enhancing the discharge efficiency of sandwich-structured polymer dielectrics at elevated temperature by building carrier blocking interface. Nano Energy, 2022, 97, 107215.	16.0	62
4	Enhancing high-temperature capacitor performance of polymer nanocomposites by adjusting the energy level structure in the micro-/meso-scopic interface region. Nano Energy, 2022, 99, 107314.	16.0	45
5	Concurrently Achieving High Discharged Energy Density and Efficiency in Composites by Introducing Ultralow Loadings of Core–Shell Structured Graphene@TiO <sub>2</sub> Nanoboxes. ACS Applied Materials & Interfaces, 2022, 14, 29292-29301.	8.0	17
6	Coldâ€sintered Na <sub>2</sub> WO <sub>4</sub> â€Ni <sub>0.2</sub> Cu <sub>0.2</sub> Zn <sub>0.6</sub> Fe <sub>2</sub> C ceramics with matched permittivity and permeability for miniaturized antenna. Journal of the American Ceramic Society, 2021, 104, 2125-2133.	) <sub>4<!--</td--><td>sub&gt; 13</td></sub>	sub> 13
7	Chemical conversion synthesis of magnetic Fe <sub>1â^'x</sub> Co <sub>x</sub> alloy nanosheets with controlled composition. Chemical Communications, 2021, 57, 2309-2312.	4.1	5
8	Additive stabilization of SEI on graphite observed using cryo-electron microscopy. Energy and Environmental Science, 2021, 14, 4882-4889.	30.8	73
9	Self-Powered Rewritable Electrochromic Display based on WO <sub>3-x</sub> Film with Mechanochemically Synthesized MoO <sub>3–<i>y</i></sub> Nanosheets. ACS Applied Materials & Interfaces, 2021, 13, 20326-20335.	8.0	46
10	Poor Stability of Li <sub>2</sub> CO <sub>3</sub> in the Solid Electrolyte Interphase of a Lithiumâ€Metal Anode Revealed by Cryoâ€Electron Microscopy. Advanced Materials, 2021, 33, e2100404.	21.0	147
11	Probing the Na metal solid electrolyte interphase via cryo-transmission electron microscopy. Nature Communications, 2021, 12, 3066.	12.8	92
12	A Facile In Situ Surfaceâ€Functionalization Approach to Scalable Laminated Highâ€Temperature Polymer Dielectrics with Ultrahigh Capacitive Performance. Advanced Functional Materials, 2021, 31, 2102644.	14.9	117
13	Asymmetric Trilayer Allâ€Polymer Dielectric Composites with Simultaneous High Efficiency and High Energy Density: A Novel Design Targeting Advanced Energy Storage Capacitors. Advanced Functional Materials, 2021, 31, 2100280.	14.9	179
14	An approach combining additive manufacturing and dielectrophoresis for 3D-structured flexible lead-free piezoelectric composites for electromechanical energy conversion. Journal of Materials Chemistry A, 2021, 9, 26767-26776.	10.3	13
15	Heterogeneous multilayer dielectric ceramics enabled by ultralowâ€temperature selfâ€constrained sintering. Journal of the American Ceramic Society, 2020, 103, 249-257.	3.8	5
16	Double core shell structured Al@Al2O3@SiO2 filled epoxy composites for thermal management application. Applied Physics Letters, 2020, 117, .	3.3	12
17	Multiscale structural engineering of dielectric ceramics for energy storage applications: from bulk to thin films. Nanoscale, 2020, 12, 17165-17184.	5.6	131
18	Self-doped tungsten oxide films induced by <i>in situ</i> carbothermal reduction for high performance electrochromic devices. Journal of Materials Chemistry C, 2020, 8, 13999-14006.	5.5	26

HONG WANG

#	Article	IF	CITATIONS
19	Ultra-high energy storage performance in lead-free multilayer ceramic capacitors <i>via</i> a multiscale optimization strategy. Energy and Environmental Science, 2020, 13, 4882-4890.	30.8	88
20	Scaling behavior and variable-range-hopping conduction of localized polarons in percolative BaTiO3-Ni0.5Zn0.5Fe2O4 ceramic composite with colossal apparent permittivity. Journal of Applied Physics, 2020, 128, .	2.5	2
21	Bioinspired Hierarchically Structured Allâ€Inorganic Nanocomposites with Significantly Improved Capacitive Performance. Advanced Functional Materials, 2020, 30, 2000191.	14.9	88
22	A highly transparent humidity sensor with fast response speed based on α-MoO <sub>3</sub> thin films. RSC Advances, 2020, 10, 25467-25474.	3.6	12
23	3D boron nitride foam filled epoxy composites with significantly enhanced thermal conductivity by a facial and scalable approach. Chemical Engineering Journal, 2020, 397, 125447.	12.7	152
24	Research progress of polymer based dielectrics for high-temperature capacitor energy storage. Wuli Xuebao/Acta Physica Sinica, 2020, 69, 217701.	0.5	10
25	High-Q (Na1-xAgx)2WO4 (x = 0.1, 0.2) ceramics with ultra-low sintering temperature. Journal of the European Ceramic Society, 2019, 39, 4156-4159.	5.7	19
26	A multifunctional smart window: detecting ultraviolet radiation and regulating the spectrum automatically. Journal of Materials Chemistry C, 2019, 7, 10446-10453.	5.5	32
27	Epoxyâ€Based Ceramicâ€Polymer Composite with Excellent Millimeterâ€Wave Broadband Absorption Properties by Facile Approach. Advanced Engineering Materials, 2019, 21, 1900981.	3.5	9
28	Ultrahigh discharge efficiency and energy density achieved at low electric fields in sandwich-structured polymer films containing dielectric elastomers. Journal of Materials Chemistry A, 2019, 7, 3729-3736.	10.3	85
29	Multilayered hierarchical polymer composites for high energydensity capacitors. Journal of Materials Chemistry A, 2019, 7, 2965-2980.	10.3	153
30	Realization of high energy density in an ultra-wide temperature range through engineering of ferroelectric sandwich structures. Nano Energy, 2019, 62, 725-733.	16.0	42
31	Temperature stable 0.35Ag2MoO4-0.65Ag0.5Bi0.5MoO4 microwave dielectric ceramics with ultra-low sintering temperatures. Journal of the European Ceramic Society, 2019, 39, 3744-3748.	5.7	13
32	Formation of antiphase boundaries in CuFe2O4 films induced by rough MgAl2O4 (001) substrates. Thin Solid Films, 2019, 680, 55-59.	1.8	7
33	Solutionâ€Processed Selfâ€Powered Transparent Ultraviolet Photodetectors with Ultrafast Response Speed for Highâ€Performance Communication System. Advanced Functional Materials, 2019, 29, 1809013.	14.9	123
34	Preparation of ultraâ€low temperature sintering ceramics with ultralow dielectric loss in Na <sub>2</sub> O– <scp>WO</scp> <sub>3</sub> binary system. Journal of the American Ceramic Society, 2019, 102, 4014-4020.	3.8	17
35	High-Temperature Dielectric Materials for Electrical Energy Storage. Annual Review of Materials Research, 2018, 48, 219-243.	9.3	540
36	Effect of the coverage level of carboxylic acids as a modifier for barium titanate nanoparticles on the performance of poly(vinylidene fluoride)-based nanocomposites for energy storage applications. Physical Chemistry Chemical Physics, 2018, 20, 6598-6605.	2.8	43

HONG WANG

#	Article	IF	CITATIONS
37	Interface thickness optimization of lead-free oxide multilayer capacitors for high-performance energy storage. Journal of Materials Chemistry A, 2018, 6, 1858-1864.	10.3	52
38	Ultrahigh energy density and greatly enhanced discharged efficiency of sandwich-structured polymer nanocomposites with optimized spatial organization. Nano Energy, 2018, 44, 364-370.	16.0	241
39	Sandwich structured poly(vinylidene fluoride)/polyacrylate elastomers with significantly enhanced electric displacement and energy density. Journal of Materials Chemistry A, 2018, 6, 24367-24377.	10.3	54
40	Multilayered ferroelectric polymer films incorporating low-dielectric-constant components for concurrent enhancement of energy density and charge–discharge efficiency. Nano Energy, 2018, 54, 288-296.	16.0	161
41	Highly Stable In-Plane Microwave Magnetism in Flexible Li <sub>0.35</sub> Zn <sub>0.3</sub> Fe <sub>2.35</sub> O <sub>4</sub> (111) Epitaxial Thin Films for Wearable Devices. ACS Applied Materials & Interfaces, 2018, 10, 32331-32336.	8.0	16
42	Simultaneously achieved temperature-insensitive high energy density and efficiency in domain engineered BaTiO3-Bi(Mg0.5Zr0.5)O3 lead-free relaxor ferroelectrics. Nano Energy, 2018, 52, 203-210.	16.0	410
43	Enhanced permittivity and permeability of (1-y)(Mg0.95Zn0.05)2TiO4-yMg0.95Zn0.05Fe2O4 ceramics. Journal of the European Ceramic Society, 2018, 38, 5367-5374.	5.7	4
44	A novel solid solution (K1-xNax)2Mo2O7 (0.0 â‰≇€‰x â‰≇€‰0.3) ceramics with ultra-low sintering Journal of the European Ceramic Society, 2018, 38, 4967-4971.	temperat	ures. 11
45	Interfacially Bound Exciton State in a Hybrid Structure of Monolayer WS <sub>2</sub> and InGaN Quantum Dots. Nano Letters, 2018, 18, 5640-5645.	9.1	29
46	Multifunctional hydrogel enables extremely simplified electrochromic devices for smart windows and ionic writing boards. Materials Horizons, 2018, 5, 1000-1007.	12.2	129
47	Compositional tailoring effect on electric field distribution for significantly enhanced breakdown strength and restrained conductive loss in sandwich-structured ceramic/polymer nanocomposites. Journal of Materials Chemistry A, 2017, 5, 4710-4718.	10.3	217
48	Tuning conductivity and magnetism of CuFe <sub>2</sub> O <sub>4</sub> via cation redistribution. RSC Advances, 2017, 7, 21926-21932.	3.6	40
49	Ultrahigh electric displacement and energy density in gradient layer-structured BaTiO <sub>3</sub> /PVDF nanocomposites with an interfacial barrier effect. Journal of Materials Chemistry A, 2017, 5, 10849-10855.	10.3	197
50	Ultrahigh Energy Storage Performance of Leadâ€Free Oxide Multilayer Film Capacitors via Interface Engineering. Advanced Materials, 2017, 29, 1604427.	21.0	247
51	The room temperature deposition of high-quality epitaxial yttrium iron garnet thin film via RF sputtering. Journal of Alloys and Compounds, 2017, 708, 213-219.	5.5	11
52	Relaxor ferroelectric 0.9BaTiO <sub>3</sub> –0.1Bi(Zn <sub>0.5</sub> Zr <sub>0.5</sub> )O <sub>3</sub> ceramic capacitors with high energy density and temperature stable energy storage properties. Journal of Materials Chemistry C, 2017, 5, 9552-9558.	5.5	241
53	Significant enhancement in breakdown strength and energy density of the BaTiO3/BaTiO3@SiO2 layered ceramics with strong interface blocking effect. Journal of the European Ceramic Society, 2017, 37, 4645-4652.	5.7	61
54	Enhanced dielectric performance of BaTiO <sub>3</sub> /PVDF composites prepared by modified process for energy storage applications. IEEE Transactions on Ultrasonics, Ferroelectrics, and Frequency Control, 2015, 62, 108-115.	3.0	69

HONG WANG

#	Article	IF	CITATIONS
55	Creation of a multilayer aluminum coating structure nanoparticle polyimide filler for electronic applications. Materials Letters, 2014, 119, 64-67.	2.6	21
56	Enhanced electric breakdown strength and high energy density of barium titanate filled polymer nanocomposites. Journal of Applied Physics, 2013, 114, 174107.	2.5	73
57	An Al@Al2O3@SiO2/polyimide composite with multilayer coating structure fillers based on self-passivated aluminum cores. Applied Physics Letters, 2013, 102, .	3.3	40
58	Polarization relaxation mechanism of Ba0.6Sr0.4TiO3/Ni0.8Zn0.2Fe2O4 composite with giant dielectric constant and high permeability. Journal of Applied Physics, 2010, 108, .	2.5	71
59	Surface functionalized Ba0.6Sr0.4TiO3 /poly(vinylidene fluoride) nanocomposites with significantly enhanced dielectric properties. Applied Physics Letters, 2009, 95, 202904.	3.3	58
60	Microstructure and Electromagnetic Properties of SrTiO <sub>3</sub> /Ni <sub>0.8</sub> Zn <sub>0.2</sub> Fe <sub>2</sub> O <sub>4</sub> Composites by Hybrid Process. Journal of the American Ceramic Society, 2009, 92, 2005-2010.	3.8	42
61	Dielectric tunability of Ba0.6Sr0.4TiO3/poly(methyl methocrylate) composites in 1-3-type structure. Applied Physics Letters, 2007, 91, .	3.3	49